Coexistence of a pseudogap and a superconducting gap for the high-T_c superconductor $La_{2-x}Sr_xCuO_4$ studied by angle-resolved photoemission spectroscopy

T. Yoshida,[1,*] W. Malaeb,[1] S. Ideta,[1] D. H. Lu,[2] R. G. Moor,[2] Z.-X. Shen,[2] M. Okawa,[3] T. Kiss,[3] K. Ishizaka,[3] S. Shin,[3] Seiki Komiya,[4] Yoichi Ando,[5] H. Eisaki,[6] S. Uchida,[1] and A. Fujimori[1]

[1]*Department of Physics, University of Tokyo, Bunkyo-ku, Tokyo 113-0033, Japan*

[2]*Department of Applied Physics and Stanford Synchrotron Radiation Laboratory, Stanford University, Stanford, California 94305, USA*

[3]*Institute of Solid State Physics, University of Tokyo, Kashiwa 277-8581, Japan*

[4]*Central Research Institute of Electric Power Industry, Yokosuka, Kanagawa 240-0196, Japan*

[5]*Institute of Scientific and Industrial Research, Osaka University, Ibaraki, Osaka 567-0047, Japan*

[6]*National Institute of Advanced Industrial Science and Technology, Tsukuba 305-8568, Japan*

(Received 12 August 2012; revised manuscript received 21 December 2015; published 19 January 2016)

The relationship between the superconducting gap and the pseudogap has been the subject of controversies. In order to clarify this issue, we have studied the superconducting gap and pseudogap of the high-T_c superconductor $La_{2-x}Sr_xCuO_4$ ($x = 0.10,14$) by angle-resolved photoemission spectroscopy (ARPES). Through the analysis of the ARPES spectra above and below T_c, we have identified a superconducting coherence peak even in the antinodal region on top of the pseudogap of a larger energy scale. The superconducting peak energy nearly follows the pure d-wave form. The d-wave order parameter Δ_0 [defined by $\Delta(k) = \Delta_0(\cos k_xa - \cos k_ya)$] for $x = 0.10$ and 0.14 are nearly the same, $\Delta_0 \sim$ 12–14 meV, leading to strong coupling $2\Delta_0/k_BT_c \sim 10$. The present result indicates that the pseudogap and the superconducting gap are distinct phenomena and can be described by the "two-gap" scenario.

DOI: 10.1103/PhysRevB.93.014513

I. INTRODUCTION

In the studies of the high-T_c cuprates, it has been a long-standing issue whether the pseudogap is related to the superconductivity or if it is a phenomenon distinct from superconductivity. Preformed Cooper pairs lacking phase coherence [1] or superconducting fluctuations [2] have been proposed as a possible origin of the pseudogap. Alternatively, the pseudogap is attributed to a competing order such as a spin density wave, charge density wave, or loop current [3]. In measurements which are sensitive to the superconducting gap around the node, such as the Andreev reflection or penetration depth, the gap decreases with underdoping [4,5], in contrast to the pseudogap which increases with underdoping, suggesting a different origin of the antinodal gap from the superconducting gap. Furthermore, photoemission [6–10] and Raman [11,12] studies have indicated the presence of two distinct energy scales. In a previous paper [13], we have pointed out that the pseudogap shows a relatively material-independent universal behavior: The pseudogap size is almost the same at the same doping level while the superconducting gap is proportional to T_c, suggesting different origins for the superconducting gap and the pseudogap. On the other hand, a simple d-wave-like gap has been also reported in some angle-resolved photoemission spectroscopy (ARPES) studies [14,15]. In such a single-gap picture, the pseudogap is interpreted as a signature of preformed Cooper pairs. Thus, the discrepancy between the experimental studies has remained.

In the analysis of the scanning tunneling microscopy (STM) spectra of single-layer cuprate $Bi_2Sr_2CuO_{6+\delta}$ (Bi2201), distinct behaviors of the superconducting gap and the pseudogap have been clearly demonstrated [16]. Even if the superconducting peak is not clearly observed in underdoped samples, the superconducting coherence peak has been identified by dividing the spectra in the superconducting state by the normal-state data. Also, a similar analysis has been done for the ARPES spectra of Bi2201 in the antinodal region and a superconducting peak has been identified [17]. These results suggest that the pseudogap and the superconducting gap have distinct origins and the superconducting gap is created on top of the electronic states with relatively broad spectral features, with a low density of states due to the pseudogap opening. As for the single-layer cuprates $La_{2-x}Sr_xCuO_4$ (LSCO), a clear superconducting peak has been identified in the off-nodal region, however, such a clear peak has not been identified in the antinodal region [9]. In order to examine the coexistence of the superconducting gap and the aforementioned pseudogap, we have performed an ARPES study of LSCO ($x = 0.14,0.10$) and analyzed the spectral line shapes to extract the signature of the superconducting peak.

II. EXPERIMENT

High-quality single crystals of LSCO ($x = 0.10$, 0.14, and 0.15) were grown by the traveling-solvent floating-zone method. The critical temperatures T_c of the $x = 0.10, 0.14$, and 0.15 samples were 28, 32, and 39 K, respectively. The ARPES measurements were carried out using synchrotron radiation at beamline 5-4 of the Stanford Synchrotron Radiation Light Source (SSRL). We used incident photons with energies of 22 eV. A Scienta R4000 spectrometer was used in the angle mode. The total energy resolution was about 7 meV. The samples were cleaved *in situ* and measurements were performed at 11 K ($< T_c$) and 40 K ($> T_c$).

[*]Present address: Graduate School of Human and Environmental Studies, Kyoto University, Sakyo-ku, Kyoto 606-8501, Japan.

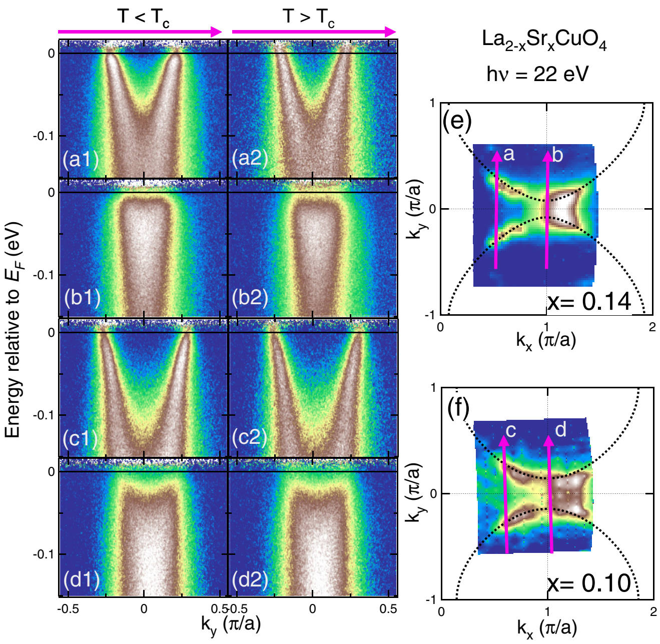

FIG. 1. ARPES spectra of LSCO with $x = 0.14$ and 0.10. (a1)–(d2) ARPES intensity plots correspond to cuts *a*–*d* in (e) and (f). The data in the left (right) have been measured below (above) T_c. Spectra have been divided by the Fermi-Dirac function convoluted with the energy resolution function. (e), (f) Intensity at E_F mapped in the k_x-k_y plane. Dotted lines illustrate Fermi surfaces.

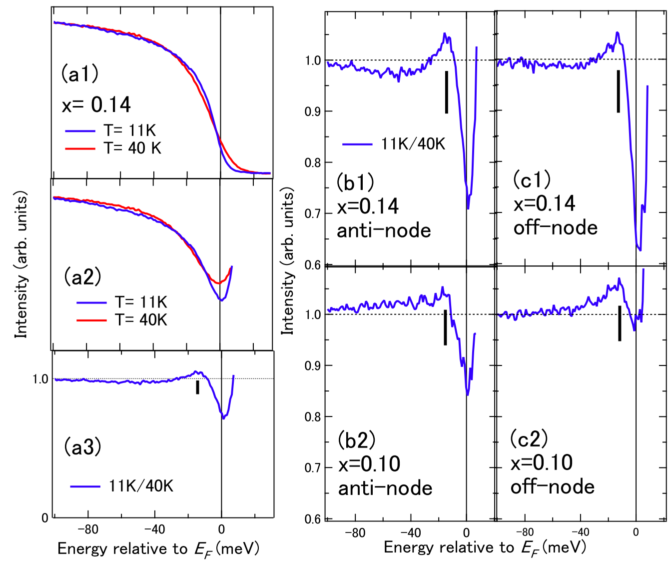

FIG. 2. Superconducting peaks observed in the ARPES spectra of LSCO with $x = 0.14$ and 0.10. (a1) Cut-integrated spectra for $x = 0.14$ for cut *b* in Fig. 1(e). (a2) Spectra in (a1) have been divided by the Fermi function convoluted with the energy resolution function. (a3) Spectra below T_c in (a2) have been divided by that above T_c. (b1)–(c2) Spectra corresponding to cuts in Fig. 1 after the above processing. Vertical bars indicate the peak positions.

III. RESULTS AND DISCUSSION

Figure 1 shows ARPES spectra of LSCO with $x = 0.14$ and 0.10 taken at $T = 11$ K ($< T_c$) and $T = 40$ K ($> T_c$). The background well away from the Fermi momenta (k_F) has been subtracted from the spectra [18]. The spectra have been divided by a convoluted Fermi-Dirac function. One can clearly see that the superconducting gap for the $x = 0.14$ sample in the off-nodal region opens below T_c [Fig. 1(a1)] and closes above T_c [Fig. 1(a2)]. The spectra for the $x = 0.10$ sample also show a similar trend, but the gap opens even above T_c, as shown in Fig. 1(c2), suggestive of a pseudogap opening. In the antinodal region, in contrast, the spectral weight near E_F is strongly suppressed even above T_c [Figs. 1(b2) and 1(d2)], indicating a pseudogap behavior. The difference between the spectra below and above T_c is not apparent. From these data, we derive the energy of the superconducting peak as described below.

In order to identify fine structures associated with the superconducting transition, we have applied a similar analysis to that employed in the previous STM [16] and ARPES studies [19] as described in Figs. 2(a1)–2(a3). First, the integrated spectrum along cut *b* in Fig. 1(a1) is divided by the Fermi-Dirac function convoluted by the energy resolution [Fig. 1(a2)]. Then, the spectrum below T_c is divided by that above T_c [Fig. 1(a3)]. As a result, we have obtained a peak-gap structure near E_F even in the antinodal region where the pseudogap dominates the spectra, indicating a superconducting peak and gap. In the same manner, the various cuts shown in Fig. 1 have been analyzed and the results are shown in Figs. 2(b1)–2(c2). Note that the obtained spectra are analogous to the tunneling spectra of *s*-wave superconductors [20] because the superconducting order parameter is approximately constant around k_F on a single cut.

Strictly speaking, the division by a convoluted Fermi-Dirac function is an approximate method to determine the gap size and one cannot exclude spurious effects due to the finite energy resolution. In order to determine more precisely the superconducting gap energy, we performed deconvolution to remove the experimental energy resolution from the cut-integrated spectra using the maximum entropy method (MEM) [21] [Fig. 3(a1)]. Then, the spectra were divided by the Fermi-Dirac function [Fig. 3(a2)]. Finally, the spectra below T_c were divided by those above T_c [Fig. 3(a3)]. In Fig. 3, we compare the processed spectra with [Figs. 3(c1) and 3(c2)] and without deconvolution [Figs. 3(b1) and 3(b2)]. Also, we have shown processed spectra (without deconvolution) for $x = 0.15$ near the node taken by the laser ARPES with a high resolution of ~2.8 meV [Fig. 3(d)]. The peak energies are plotted as a function of the *d*-wave parameter $[\cos(k_x) - \cos(k_y)]/2$ in Fig. 3(e) and compared with the previous result of $x = 0.15$, which shows "two-gap" behavior [13]. Note that the peak positions of the deconvoluted spectra are closer to E_F by ~5 meV than those without deconvolution, nearly following the pure *d* wave from the nodal to the antinodal regions [13]. Furthermore, the gap sizes in the off-nodal region for both the $x = 0.14$ and 0.10 samples are almost the same, in contrast to the previous ARPES study of LSCO [22]. The observed *d*-wave-like gap in the antinodal region $\Delta_0 \sim 12$–14 meV gives a strong coupling ratio $2\Delta_0/k_BT_c \sim 10$, similar to the previous Bi2201 result [17]. The nearly constant Δ_0 from the optimally doped to underdoped regions is consistent with the recent results in $Bi_2Sr_2CaCu_2O_{8+\delta}$ (Bi2212) [23] with

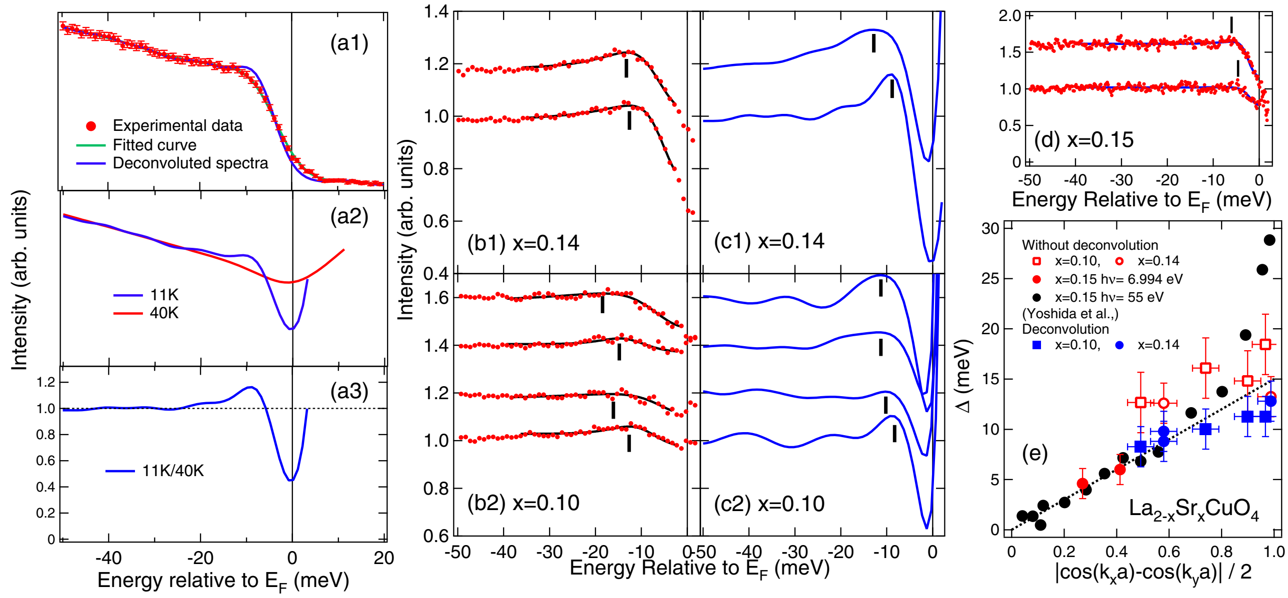

FIG. 3. Angular dependence of the superconducting peaks obtained from ARPES spectra of LSCO with $x = 0.14$ and 0.10. (a1) Cut-integrated spectrum for $x = 0.14$ in the off-nodal direction taken at 11 K and its deconvoluted spectrum using the MEM. Fitted curves produced by the MEM well reproduce the original experimental data. (a2) Deconvoluted spectra divided by the Fermi-Dirac function. (a3) Spectrum obtained by dividing the 11 K data ($< T_c$) by the 40 K data ($> T_c$) in (a2). (b1), (b2) Superconducting peak obtained in Figs. 2(c1) and 2(c2). The spectra in (b1) and (b2) have been deconvoluted with the energy resolution using the MEM. (d) Superconducting gap near the nodal direction for $x = 0.15$ taken at $h\nu = 6.994$ eV using a UV laser at the Institute of Solid State Physics (ISSP), the University of Tokyo. The data were analyzed in the same manner as in (b1) and (b2). (e) Angular dependences of the superconducting peak are plotted as a function of d-wave parameter $|\cos(k_x) - \cos(k_y)|/2$. For comparison, previous results of the gap for $x = 0.15$ are also plotted.

larger $T_c > 90$ K, indicating universal behavior in the high-T_c cuprates.

Here, we shall discuss differences in the "two-gap" behavior between the single-layer and bilayer cuprates. In the single-layer cuprates such as LSCO and Bi2201, the coexistence of the pseudogap and the superconducting peak in the antinodal direction has been revealed by the ARPES [19] and STM studies [24,25], including the present result. However, in the case of Bi2212 [6,7], such two energy scales have not been resolved in the antinodal spectra. Only a single-peak structure appears below T_c in the optimally doped and underdoped regions. The different behaviors between the single- and double-layer cuprates can be understood as follows: When the pseudogap has a different origin from the superconducting gap, the superconducting peak is created on the pseudogap feature of the broad incoherent spectral weight.

Figure 4 shows the doping dependences of Δ^*, Δ_0, and T^* for LSCO and Bi2201 as well as those for double-layer Bi2212 (inset). Here, the antinodal gap Δ^* is defined by the peak energy in the antinodal region [13] and T^* is the pseudogap temperature. As shown in the figure, in the single-layer cuprates, which have relatively low T_c's, the energy scale of the superconducting (SC) gap is smaller than that of the pseudogap and the T_c is lower than the pseudogap temperature T^* in the optimally doped and the underdoped region. Therefore, the superconducting gap appears below T_c within the pseudogap which is created below T^*, resulting in the two energy scales in the spectral weight distribution. On the other hand, in the bilayer cuprates Bi2212, which have a relatively high T_c comparable to T^*, both energy scales are comparable and T_c

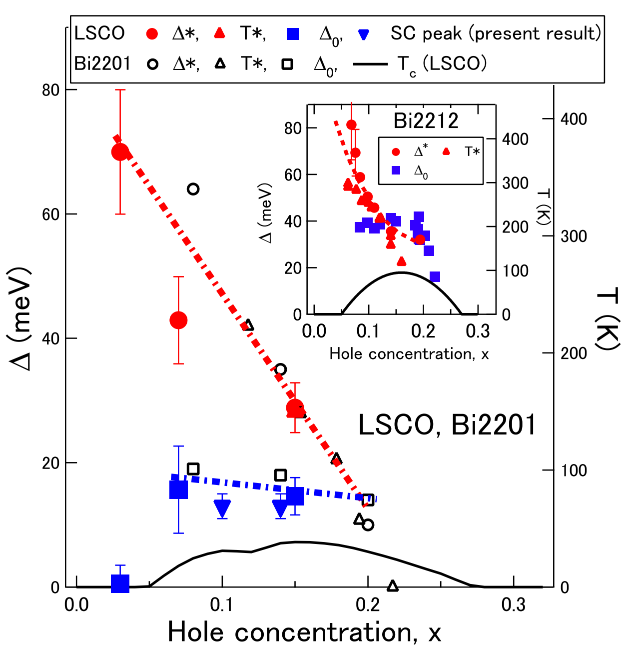

FIG. 4. Doping dependences of the characteristic energies (Δ^*, Δ_0 [13,35,36]) and temperatures (T^*, T_c) for the single-layer cuprates (LSCO, Bi2201). The antinodal gap Δ^* is defined by the energy of the hump or peak in the antinodal region [36]. Parameter values have been taken from Ref. [36] and references therein. The present LSCO result of the SC peak energy in the antinode direction is also plotted. The inset shows those for the double-layer cuprates Bi2212. Gap energies Δ and temperatures T have been scaled as $2\Delta = 4.3k_BT$ in these plots.

and T^* are also comparable in the optimally doped region (see the inset in Fig. 4). Because the pseudogap has a comparable energy scale with the superconducting gap Δ_0 and opens at nearly the same temperatures, the two gaps cannot be clearly resolved. Thus, the superconducting peak may show only a weak deviation from the pure d wave in Bi2212 [6,7], unlike the strong deviation with two-energy scales in the single-layer cuprates [8,9,13].

The present study has revealed that the superconducting gap has a nearly pure d-wave form and exists even in the antinodal direction in the optimally doped to underdoped region. A phenomenological model for the two-gap state proposed by Yang, Rice, and Zhang (YRZ) well accords with the present coexistence of the superconducting and the pseudogap [26]. While YRZ assumes a resonating valence bond (RVB) gap as the antinodal gap, there are several possible candidates for the origin of the pseudogap. Calculations assuming an order parameter different from the superconductivity, such as valence bond glass [27] and the spin-density wave (SDW) state [28], have predicted that the superconducting gap persists beyond the end of the Fermi arc all the way to the antinode, in accordance with the present observation. Particularly, in the SDW-based calculation [28], a humplike pseudogap and a sharp superconducting peak in the antinodal direction as seen in the present result have been reproduced. A temperature-dependent ARPES study reveals particle-hole asymmetry of the antinodal gap, most likely due to the density-wave gap formation [29]. This observation would be related to the charge ordered state observed in STM [30] or stripe formation [31]. From STM results of the charge order [24,32], the pseudogap in the antinodal region is most likely to link to such a two-dimensional electronic charge order.

IV. CONCLUSION

We have identified the superconducting peak LSCO ($x = 0.10, 0.14$) in the antinodal region from an analysis of the ARPES spectra above and below T_c. The superconducting peaks follow the pure d wave on top of the pseudogap of a larger energy scale. The d-wave gap parameters Δ_0 of the optimally and underdoped samples are nearly the same, similar to the Bi2212 results [23], indicating universal behavior in the high-T_c cuprates. Since the superconducting order parameter is nearly doping independent in the underdoped region, the drop of T_c with underdoping is due to the decreasing length of the Fermi arc. The present results have reinforced that the pseudogap and the superconducting gap are distinct phenomena.

ACKNOWLEDGMENTS

We are grateful to H. Ding for informative discussions. This work was supported by a Grant-in-Aid for Young Scientists (B) and the Japan-China-Korea A3 Foresight Program from the Japan Society for the Promotion of Science. SSRL is operated by the Department of Energy's Office of Basic Energy Science, Division of Chemical Sciences and Material Sciences.

[1] V. J. Emery and S. A. Kivelson, Nature (London) **374**, 434 (1995).
[2] J. R. Engelbrecht, A. Nazarenko, M. Randeria, and E. Dagotto, Phys. Rev. B **57**, 13406 (1998).
[3] M. E. Simon and C. M. Varma, Phys. Rev. Lett. **89**, 247003 (2002).
[4] G. Deustcher, Nature (London) **397**, 410 (1999).
[5] C. Panagopoulos, J. R. Cooper, and T. Xiang, Phys. Rev. B **57**, 13422 (1998).
[6] K. Tanaka, W. S. Lee, D. H. Lu, A. Fujimori, T. Fujii, Risdiana, I. Terasaki, D. J. Scalapino, T. P. Devereaux, Z. Hussain, and Z.-X. Shen, Science **314**, 1910 (2006).
[7] W. S. Lee, I. M. Vishik, K. Tanaka, D. H. Lu, T. Sasagawa, N. Nagaosa, T. P. Devereaux, Z. Hussain, and Z.-X. Shen, Nature (London) **450**, 81 (2007).
[8] T. Kondo, T. Takeuchi, A. Kaminski, S. Tsuda, and S. Shin, Phys. Rev. Lett. **98**, 267004 (2007).
[9] K. Terashima, H. Matsui, T. Sato, T. Takahashi, M. Kofu, and K. Hirota, Phys. Rev. Lett. **99**, 017003 (2007).
[10] M. Hashimoto, T. Yoshida, K. Tanaka, A. Fujimori, M. Okusawa, S. Wakimoto, K. Yamada, T. Kakeshita, H. Eisaki, and S. Uchida, Phys. Rev. B **75**, 140503(R) (2007).
[11] M. Opel, R. Nemetschek, C. Hoffmann, R. Philipp, P. F. Müller, R. Hackl, I. Tüttö, A. Erb, B. Revaz, E. Walker, H. Berger, and L. Forró, Phys. Rev. B **61**, 9752 (2000).
[12] M. L. Tacon, A. Sacuto, A. Georges, G. Kotliar, Y. Gallais, D. Colson, and A. Forget, Nat. Phys. **2**, 537 (2006).
[13] T. Yoshida, M. Hashimoto, S. Ideta, A. Fujimori, K. Tanaka, N. Mannella, Z. Hussain, Z.-X. Shen, M. Kubota, K. Ono, S. Komiya, Y. Ando, H. Eisaki, and S. Uchida, Phys. Rev. Lett. **103**, 037004 (2009).
[14] J. Meng, W. Zhang, G. Liu, L. Zhao, H. Liu, X. Jia, W. Lu, X. Dong, G. Wang, H. Zhang, Y. Zhou, Y. Zhu, X. Wang, Z. Zhao, Z. Xu, C. Chen, and X. J. Zhou, Phys. Rev. B **79**, 024514 (2009).
[15] M. Shi, A. Bendounan, E. Razzoli, S. Rosenkranz, M. R. Norman, J. C. Campuzano, J. Chang, M. Mansson, Y. Sassa, T. Claesson, O. Tjernberg, L. Patthey, N. Momono, M. Oda, M. Ido, S. Guerrero, C. Mudry, and J. Mesot, Europhys. Lett. **88**, 27008 (2009).
[16] M. C. Boyer, W. D. Wise, K. Chatterjee, M. Yi, T. Kondo, T. Takeuchi, H. Ikuta, and E. W. Hudson, Nat. Phys. **3**, 802 (2007).
[17] J.-H. Ma, Z.-H. Pan, F. C. Niestemski, M. Neupane, Y.-M. Xu, P. Richard, K. Nakayama, T. Sato, T. Takahashi, H.-Q. Luo, L. Fang, H.-H. Wen, Z. Wang, H. Ding, and V. Madhavan, Phys. Rev. Lett. **101**, 207002 (2008).
[18] M. Hashimoto, R.-H. He, I. M. Vishik, F. Schmitt, R. G. Moore, D. H. Lu, Y. Yoshida, H. Eisaki, Z. Hussain, T. P. Devereaux, and Z.-X. Shen, Phys. Rev. B **86**, 094504 (2012).
[19] H. Ding, J. R. Engelbrecht, Z. Wang, J. C. Campuzano, S.-C. Wang, H.-B. Yang, R. Rogan, T. Takahashi, K. Kadowaki, and D. G. Hinks, Phys. Rev. Lett. **87**, 227001 (2001).
[20] W. L. McMillan and J. M. Rowell, Phys. Rev. Lett. **14**, 108 (1965).
[21] The MEM has been used to numerically deconvolute an image or spectrum which has been convoluted by some function. In the deconvolution process, the generalized entropy is defined in order to overcome the numerical instability. In previous ARPES

studies, the Eliashberg function has been extracted from the ARPES data by the MEM [33,34].

[22] M. Shi, J. Chang, S. Pailhés, M. R. Norman, J. C. Campuzano, M. Månsson, T. Claesson, O. Tjernberg, A. Bendounan, L. Patthey, N. Momono, M. Oda, M. Ido, C. Mudry, and J. Mesot, Phys. Rev. Lett. **101**, 047002 (2008).

[23] I. M. Vishik, M. Hashimoto, R.-H. He, W.-S. Lee, F. Schmitt, D. Lu, R. G. Moore, C. Zhang, W. Meevasana, T. Sasagawa, S. Uchida, K. Fujita, S. Ishida, M. Ishikado, Y. Yoshida, H. Eisaki, Z. Hussain, T. P. Devereaux, and Z.-X. Shen, Proc. Natl. Acad. Sci. USA **109**, 18332 (2012).

[24] T. Kurosawa, T. Yoneyama, Y. Takano, M. Hagiwara, R. Inoue, N. Hagiwara, K. Kurusu, K. Takeyama, N. Momono, M. Oda, and M. Ido, Phys. Rev. B **81**, 094519 (2010).

[25] Y. He, Y. Yin, M. Zech, A. Soumyanarayanan, M. M. Yee, T. Williams, M. C. Boyer, K. Chatterjee, W. D. Wise, I. Zeljkovic, T. Kondo, T. Takeuchi, H. Ikuta, P. Mistark, R. S. Markiewicz, A. Bansil, S. Sachdev, E. W. Hudson, and J. E. Hoffman, Science **344**, 608 (2014).

[26] K.-Y. Yang, T. M. Rice, and F.-C. Zhang, Phys. Rev. B **73**, 174501 (2006).

[27] L. R. Niestemski and Z. Wang, Phys. Rev. Lett. **102**, 107001 (2009).

[28] T. Das, R. S. Markiewicz, and A. Bansil, Phys. Rev. B **77**, 134516 (2008).

[29] M. Hashimoto, R.-H. He, K. Tanaka, J.-P. Testaud, W. Meevasana, R. G. Moore, D. Lu, H. Yao, Y. Yoshida, H. Eisaki, T. P. Devereaux, Z. Hussain, and Z.-X. Shen, Nat. Phys. **6**, 414 (2010).

[30] T. Hanaguri, C. Lupien, Y. Kohsaka, D.-H. Lee, M. Azuma, M. Takano, H. Takagi, and J. C. Davis, Nature (London) **430**, 1001 (2004).

[31] J. M. Tranquada, B. J. Sternlieb, J. D. Axe, Y. Nakamura, and S. Uchida, Nature (London) **375**, 561 (1995).

[32] E. H. da Silva Neto, P. Aynajian, A. Frano, R. Comin, E. Schierle, E. Weschke, A. Gyenis, J. Wen, J. Schneeloch, Z. Xu, S. Ono, G. Gu, M. Le Tacon, and A. Yazdani, Science **343**, 393 (2014).

[33] J. Shi, S.-J. Tang, B. Wu, P. T. Sprunger, W. L. Yang, V. Brouet, X. J. Zhou, Z. Hussain, Z.-X. Shen, Z. Zhang, and E. W. Plummer, Phys. Rev. Lett. **92**, 186401 (2004).

[34] X. J. Zhou, J. Shi, T. Yoshida, T. Cuk, W. L. Yang, V. Brouet, J. Nakamura, N. Mannella, S. Komiya, Y. Ando, F. Zhou, W. X. Ti, J. W. Xiong, Z. X. Zhao, T. Sasagawa, T. Kakeshita, H. Eisaki, S. Uchida, A. Fujimori, Z. Zhang, E. W. Plummer, R. B. Laughlin, Z. Hussain, and Z.-X. Shen, Phys. Rev. Lett. **95**, 117001 (2005).

[35] S.-i. Ideta, T. Yoshida, A. Fujimori, H. Anzai, T. Fujita, A. Ino, M. Arita, H. Namatame, M. Taniguchi, Z.-X. Shen, K. Takashima, K. Kojima, and S.-i. Uchida, Phys. Rev. B **85**, 104515 (2012).

[36] T. Yoshida, M. Hashimoto, I. M. Vishik, Z.-X. Shen, and A. Fujimori, J. Phys. Soc. Jpn. **81**, 011006 (2012).